An Optimal Frequency in Ca^{2+} Oscillations for Stomatal Closure Is an Emergent Property of Ion Transport in Guard Cells[1][CC-BY]

Carla Minguet-Parramona[2], Yizhou Wang[2], Adrian Hills, Silvere Vialet-Chabrand, Howard Griffiths, Simon Rogers, Tracy Lawson, Virgilio L. Lew*, and Michael R. Blatt*

Laboratory of Plant Physiology and Biophysics, University of Glasgow, Bower Building, Glasgow G12 8QQ, United Kingdom (C.M.-P., Y.W., A.H., M.R.B.); Biological Sciences, University of Essex, Wivenhoe Park, Colchester CO4 3SQ, United Kingdom (S.V.-C., T.L.); Plant Sciences, University of Cambridge, Downing Street, Cambridge CB2 3EA, United Kingdom (H.G.); Computing Science, University of Glasgow, Alwyn Williams Building, Glasgow G12 8QQ, United Kingdom (S.R.); and Physiological Laboratory, University of Cambridge, Downing Street, Cambridge CB2 3EG, United Kingdom (V.L.L.)

ORCID IDs: 0000-0002-2188-383X (Y.W.); 0000-0003-3578-4477 (S.R.).

Oscillations in cytosolic-free Ca^{2+} concentration ($[Ca^{2+}]_i$) have been proposed to encode information that controls stomatal closure. $[Ca^{2+}]_i$ oscillations with a period near 10 min were previously shown to be optimal for stomatal closure in Arabidopsis (*Arabidopsis thaliana*), but the studies offered no insight into their origins or mechanisms of encoding to validate a role in signaling. We have used a proven systems modeling platform to investigate these $[Ca^{2+}]_i$ oscillations and analyze their origins in guard cell homeostasis and membrane transport. The model faithfully reproduced differences in stomatal closure as a function of oscillation frequency with an optimum period near 10 min under standard conditions. Analysis showed that this optimum was one of a range of frequencies that accelerated closure, each arising from a balance of transport and the prevailing ion gradients across the plasma membrane and tonoplast. These interactions emerge from the experimentally derived kinetics encoded in the model for each of the relevant transporters, without the need of any additional signaling component. The resulting frequencies are of sufficient duration to permit substantial changes in $[Ca^{2+}]_i$ and, with the accompanying oscillations in voltage, drive the K^+ and anion efflux for stomatal closure. Thus, the frequency optima arise from emergent interactions of transport across the membrane system of the guard cell. Rather than encoding information for ion flux, these oscillations are a by-product of the transport activities that determine stomatal aperture.

Stomata in the leaf epidermis are the main pathway both for CO_2 entry for photosynthesis and for foliar water loss by transpiration. Guard cells surround the stomatal pore and regulate the aperture, balancing the often conflicting demands for CO_2 and water conservation. Guard cells open and close the pore by expanding and contracting through the uptake and loss, respectively, of osmotic solutes, notably of K^+, Cl^-, and malate^{2-} (Mal^{2-}; Pandey et al., 2007; Kim et al., 2010; Roelfsema and Hedrich, 2010; Lawson and Blatt, 2014). These transport processes comprise the final effectors of a regulatory network that coordinates transport across the plasma membrane and tonoplast, and maintains the homeostasis of the guard cell. A number of well-defined signals—including light, CO_2, drought and the water stress hormone abscisic acid (ABA)—act on this network, altering transport, solute content, turgor and cell volume, and ultimately stomatal aperture.

Much research has focused on stomatal closure, underscoring both Ca^{2+}-independent and Ca^{2+}-dependent signaling. Of the latter, elevated cytosolic-free Ca^{2+} concentration ($[Ca^{2+}]_i$) inactivates inward-rectifying K^+ channels ($I_{K,in}$) to prevent K^+ uptake and activates Cl^- (anion) channels (I_{Cl}) at the plasma membrane to depolarize the membrane and engage K^+ efflux through outward-rectifying K^+ channels ($I_{K,out}$; Keller et al., 1989; Blatt et al., 1990; Thiel et al., 1992; Lemtiri-Chlieh and MacRobbie, 1994). ABA, and most likely CO_2 (Kim et al.,

[1] This work was supported by the Biotechnology and Biological Sciences Research Council (grant nos. BB/L019205/1 and BB/M001601/1 to M.R.B., BB/L001276/1 to M.R.B. and S.R., and BB/I001187/1 to H.G. and T.L.) and EU OPTIMA (project 289642 Ph.D. studentship to C.M.-P.).

[2] These authors contributed equally to the article.

* Address correspondence to michael.blatt@glasgow.ac.uk and vll1@cam.ac.uk.

The author responsible for distribution of materials integral to the findings presented in this article in accordance with the policy described in the Instructions for Authors (www.plantphysiol.org) is: Michael R. Blatt (michael.blatt@glasgow.ac.uk).

C.M.-P. and Y.W. tested OnGuard models, quantifying and validating the outputs; A.H. developed OnGuard and Fourier analysis routines for output analysis; S.V.-C., H.G., S.R., and T.L. contributed to discussion of output and Fourier analysis; M.R.B. developed the concepts and carried out the Fourier analysis; V.L.L. and M.R.B. wrote the article.

www.plantphysiol.org/cgi/doi/10.1104/pp.15.01607

2010), elevate $[Ca^{2+}]_i$ by facilitating Ca^{2+} entry at the plasma membrane to trigger Ca^{2+} release from endomembrane stores, a process often described as Ca^{2+}-induced Ca^{2+} release (Grabov and Blatt, 1998, 1999). The hormone promotes Ca^{2+} influx by activating Ca^{2+} channels (I_{Ca}) at the plasma membrane, even in isolated membrane patches (Hamilton et al., 2000, 2001), which is linked to reactive oxygen species (Kwak et al., 2003; Wang et al., 2013). In parallel, cADP-ribose and nitric oxide promote endomembrane Ca^{2+} release and $[Ca^{2+}]_i$ elevation (Leckie et al., 1998; Neill et al., 2002; Garcia-Mata et al., 2003; Blatt et al., 2007). Best estimates indicate that endomembrane release accounts for more than 95% of the Ca^{2+} entering the cytosol to raise $[Ca^{2+}]_i$ (Chen et al., 2012; Wang et al., 2012).

One feature of stomatal response to ABA, and indeed to a range of stimuli both hormonal as well as external, is its capacity for oscillations both in membrane voltage and $[Ca^{2+}]_i$. Guard cell $[Ca^{2+}]_i$ at rest is typically around 100 to 200 nM, as it is in virtually all living cells. In response to ABA, $[Ca^{2+}]_i$ can rise above 1 μM—and locally, most likely above 10 μM—often in cyclic transients of tens of seconds to several minutes' duration in association with oscillations in voltage and stomatal closure (Gradmann et al., 1993; McAinsh et al., 1995; Webb et al., 1996; Grabov and Blatt, 1998, 1999; Staxen et al., 1999; Allen et al., 2001). In principle, cycling in voltage and $[Ca^{2+}]_i$ arises as closure is accelerated with a controlled release of K^+, Cl^-, and Mal^{2-} from the guard cell and is subject to extracellular ion concentrations (Gradmann et al., 1993; Chen et al., 2012). However, it has been proposed that these, and similar oscillations in a variety of plant cell models, serve as physiological signals in their own right (McAinsh et al., 1995; Ehrhardt et al., 1996; Taylor et al., 1996). In support of such a signaling role, experiments designed to impose $[Ca^{2+}]_i$ (and voltage) oscillations in guard cells have yielded an optimal frequency for closure with a period near 10 min (Allen et al., 2001). Nonetheless, the studies offer no mechanistic explanation for this optimum that could validate a causal role in signaling, and none has been forthcoming since. Here we address questions of how such optimal frequencies in $[Ca^{2+}]_i$ oscillation arise and their relevance for stomatal closure, using quantitative systems analysis of guard cell transport and homeostasis. Our findings indicate that oscillations in voltage and $[Ca^{2+}]_i$, and their optima associated with stomatal closure, are most simply explained as emerging from the interactions between ion transporters that drive stomatal closure. Thus, we conclude that these oscillations do not control, but are a by-product of the transport that determines stomatal aperture.

RESULTS

Figure 1, A to C, shows the model outputs for voltage, $[Ca^{2+}]_i$ and aperture at times late in the daylight period of the simulated diurnal cycle when the stomata close (Chen et al., 2012; Wang et al., 2012). The overview illustrates the onset of oscillations, initially as rapid transitions in voltage—and coupled, but limited oscillations in $[Ca^{2+}]_i$—with a gradual shift over roughly 1.5 h as these transients contract and accelerate. The oscillations culminate with long membrane depolarizations and hyperpolarizations, each of several minutes' duration, accompanied by large transients in $[Ca^{2+}]_i$ from a baseline near 200 nM to values in excess of 1 μM. This entire sequence of oscillations is stably repeated with each diurnal cycle for any given set of model parameters (Chen et al., 2012). At their onset, the voltage transients initially traverse a range of approximately 50 mV with a cycle period near 0.3 min. These oscillations, and the accompanying variations in $[Ca^{2+}]_i$, are clipped in a saw-tooth pattern (Fig. 1D). The subsequent, long voltage oscillations, by contrast, traverse roughly 100 mV, show more extensive relaxations and dwell times at each voltage extreme, and are closely matched by long cycles of $[Ca^{2+}]_i$ elevation and recovery in which $[Ca^{2+}]_i$ rises and then decays as Ca^{2+} release is followed by its sequestration and export from the cytosol (Chen et al., 2012). In effect, these extended time periods are long enough to permit the rise and fall in $[Ca^{2+}]_i$ to "catch up" with the voltage cycle. Fourier analysis of the oscillations in voltage and $[Ca^{2+}]_i$ (Fig. 1E) showed a range of oscillation frequencies between 0.3 and 2 mHz, and resonance frequencies near 3.5, 6, 7, and 9 mHz. The latter series is most evident in the $[Ca^{2+}]_i$ oscillations, as is to be expected from the nonsinusoidal waveform in $[Ca^{2+}]_i$. The major peaks of both voltage and $[Ca^{2+}]_i$ align with one another, confirming their close association, and the spread between approximately 0.3 mHz and the major peak at 1.9 mHz (=8.9 min) suggests complex relationships originating with the ensemble of transport activities within the cell, an interpretation that was drawn previously from observing the interactions between the several transporters in simulation (Chen et al., 2012).

It is clear from Figure 1 that the consequence of both the short and long oscillations was to promote solute loss and stomatal closure in simulation. For the long oscillations, the effect was a step-wise decay in aperture with bursts of rapid closure separated by periods in which there is little change in aperture. However, even the short oscillations in voltage and $[Ca^{2+}]_i$ associated with periods of solute loss and small declines in aperture. Most striking is the difference in rates of stomatal closure with the expanded cycles in voltage and $[Ca^{2+}]_i$. Figure 2 summarizes the closure rate as a function of oscillation period. To avoid the potential complication of the changing solute gradients, the rates of closure here are corrected in inverse ratio with the decline in the sum of the thermodynamic driving forces for K^+ and anion flux. This correction has no qualitative effect on the overall pattern. Remarkably, the results showed that closure followed a sharp, biphasic function of oscillation frequency with a maximum closure rate at a cycle period of 8.9 min (=1.9 mHz). Closure rate fell off steeply to either side of this value, with a plateau in rates at longer cycle periods. Also plotted is the

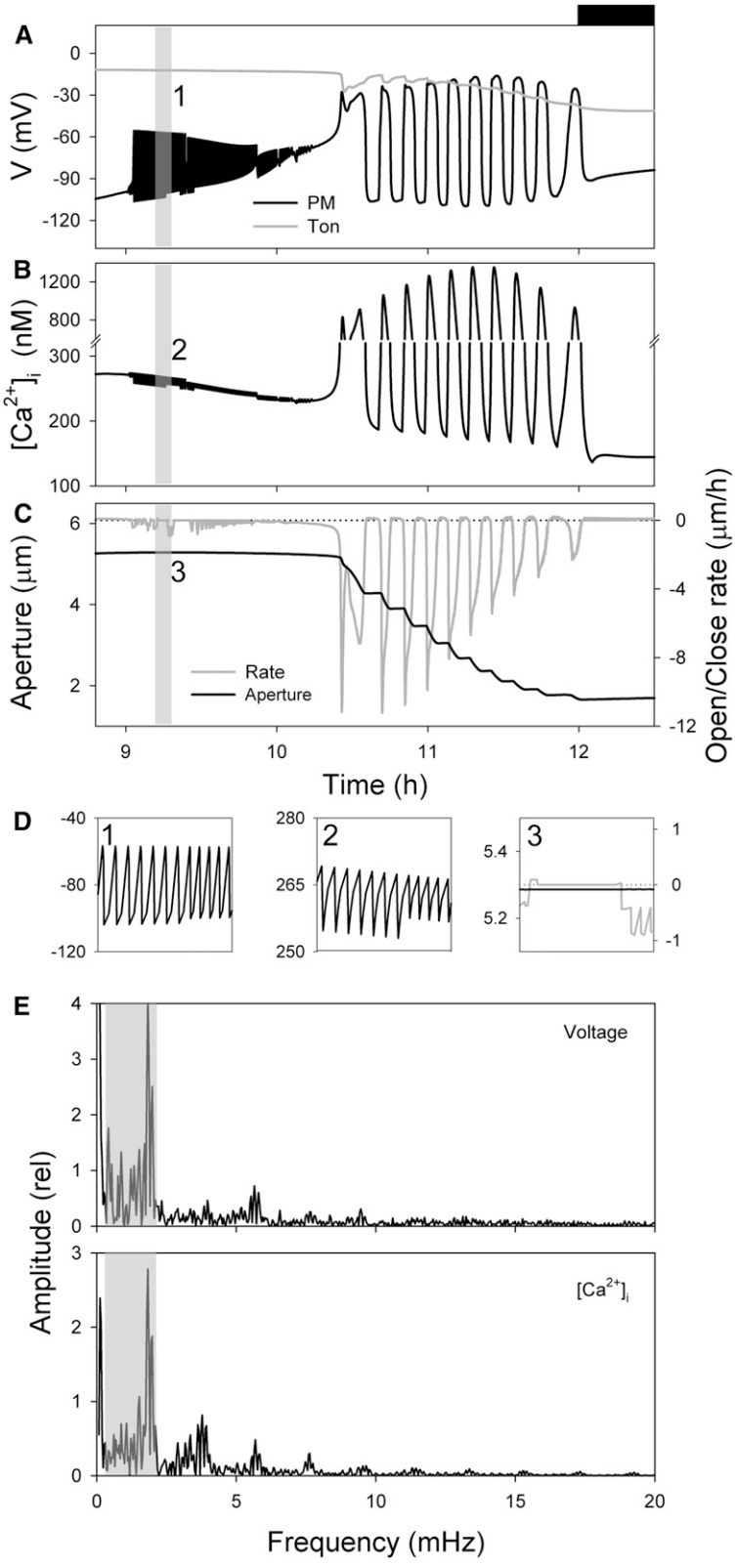

Figure 1. Macroscopic outputs of the OnGuard Arabidopsis model. Outputs resolved over a standard diurnal cycle (12 h light:12 h dark; dark period indicated by bar above) with 10 mM KCl, 1 mM $CaCl_2$, and pH 6.5 outside. The full set of model parameters and initializing variables will be found in Wang et al. (2012) and may be downloaded with the OnGuard software at www.psrg.org.uk. A to C, Outputs for the diurnal period 8.8 to 12.5 h from the start of the diurnal cycle (dark period indicated by bar above) for plasma membrane and tonoplast voltage (A), $[Ca^{2+}]_i$ (B), and stomatal aperture and

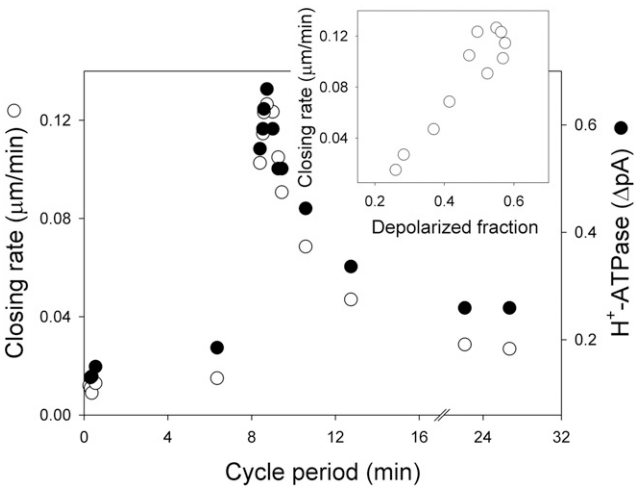

Figure 2. Aperture closing rate as a function of the oscillation cycle period. Data from Figure 1 for each of the long oscillatory cycles and from a selection of the early, rapid cycles are plotted together with H^+-ATPase current dynamics. H^+-ATPase current determined as the difference in current at 0 mV between the hyperpolarized and depolarized phases of each oscillation cycle. Closing rates shown are corrected proportionally for the decay in K^+ and anion electrochemical driving force during closure, which elevated the closing rates by approximately 20% to 25% for cycle periods of 10 min and longer. Inset, Closing rate as a function of the relative time fraction spent in the depolarized phase of the oscillation cycle. Note the slight hysteresis loop near the maximum rates of closure.

relationship of closure rate with the time fraction in the depolarized phase of the cycle. Maximum rate associated with a mean time fraction around 0.50 to 0.55 in the depolarized phase, in other words rapid closure occurred with a near-symmetric cycle of elevated $[Ca^{2+}]_i$ (depolarized voltage) and resting $[Ca^{2+}]_i$ (hyperpolarized voltage). These characteristics match closely those previously identified in experiments: Allen et al. (2001) reported maximum closure with an imposed $[Ca^{2+}]_i$ oscillation frequency near 10 min and a mean time fraction of 0.5 in the depolarized phase. In short, the model reproduces these phenomenological observations faithfully, without ad hoc manipulation or refinements in any of the system parameters.

To gain a better understanding of the drivers behind this optimum in closure rate, we examined the activities of the plasma membrane H^+- and Ca^{2+}-ATPases, as well as the $I_{K,in}$, $I_{K,out}$, I_{Ca}, I_{Cl}, and ALMT Mal^{2-} channels at the plasma membrane. Figure 3 shows cycle period as a function of the plasma membrane currents carried by the H^+-ATPase, the Ca^{2+}-ATPase, and each of the predominant channels known to integrate with the voltage and $[Ca^{2+}]_i$ oscillations. A corresponding analysis for the tonoplast VH^+-ATPase, VH^+-PPase, and Ca^{2+}-ATPase, as well as the major tonoplast K^+ and anion channels, is included in Supplemental Figure S1. Currents in each case were determined at the oscillation cycle limits and at fixed voltages outside the range in which the transporters are sensitive to voltage itself. The approach therefore avoids the complications of kinetic limitation by voltage and $[Ca^{2+}]_i$. Thus, for the H^+-ATPase, for example, the current was determined for 0 mV, at which the pump is essentially independent of membrane voltage and close to its positive maximum output, and when the free-running voltage was at its most negative, that corresponds to low $[Ca^{2+}]_i$ values near 200 nM, so minimizing its interference. It is obvious that oscillations in the model were closely tied to plasma membrane H^+-ATPase and, to a lesser extent, to tonoplast VH^+-ATPase activity. An association with the VH^+-ATPase is consistent with experimental evidence that the *det3* mutant, which suppresses this transporter, also eliminates Ca^{2+}-evoked oscillations and stomatal closure (Allen et al., 2000). No strong dependence on Ca^{2+}-ATPases, VH^+-PPase, or the various ion channel activities was evident. The results also indicated that the H^+-ATPase activity must decline substantially in order to facilitate the slow oscillations and accelerate stomatal closure, an observation in agreement with studies of the *ost2* H^+-ATPase mutant that remains constitutively active and prevents stomatal closure (Merlot et al., 2007 and below).

With the exception of the outward-rectifying K^+ channel, all of these transporters are sensitive to $[Ca^{2+}]_i$. The H^+-ATPase, especially, is strongly suppressed by $[Ca^{2+}]_i$ elevation (Kinoshita et al., 1995; Chen et al., 2012; Hills et al., 2012). Therefore, to explore how critically stomatal closure rate correlated with $[Ca^{2+}]_i$, we plotted the dynamic variation in plasma membrane H^+-ATPase activity together with closing rate as a function of cycle period (Fig. 2). A close match was found between these two variables, indicating that the $[Ca^{2+}]_i$-driven feedback on the H^+-ATPase features strongly in the link between cycle period and stomatal closure rates. The observation is important, because the plasma membrane H^+-ATPase, the tonoplast VH^+-ATPase and VH^+-PPase, and the Ca^{2+}-ATPases are all moderated externally in simulation, their activities declining with the daylight (Blatt et al., 2014; Wang et al., 2014). Yet only the H^+-ATPase and the VH^+-ATPase activities showed

Figure 1. (*Continued.*)
the rate of opening/closing in stomatal aperture (C; =ΔAperture/Δt). Positive rates here indicate opening, and negative rates indicate closing. D, Expanded view of the rapid cycles in voltage, $[Ca^{2+}]_i$, aperture, and the rates of opening/closing corresponding to the period (9.2–9.3 h) highlighted by the gray bars in A to C cross-referenced by numbers. Note the periodic, step-like decrease in aperture and its association with the periods of membrane depolarization and elevated $[Ca^{2+}]_i$. Trials with diurnal fluence rates weighted to peak at 2, 6, or 10 h yielded a comparable series of oscillations, indicating that the kinetics of decay in primary ATP-dependent transport have no substantive influence on this behavior. E, Fourier spectral analysis of oscillation frequencies in voltage and $[Ca^{2+}]_i$ for the data in A to C. The plots show the relative amplitude of the component frequencies. Frequencies within the gray bars correspond to periodicities of approximately 6 to 26 min and show a prominent amplitude at 8.9 min (=1.9 mHz).

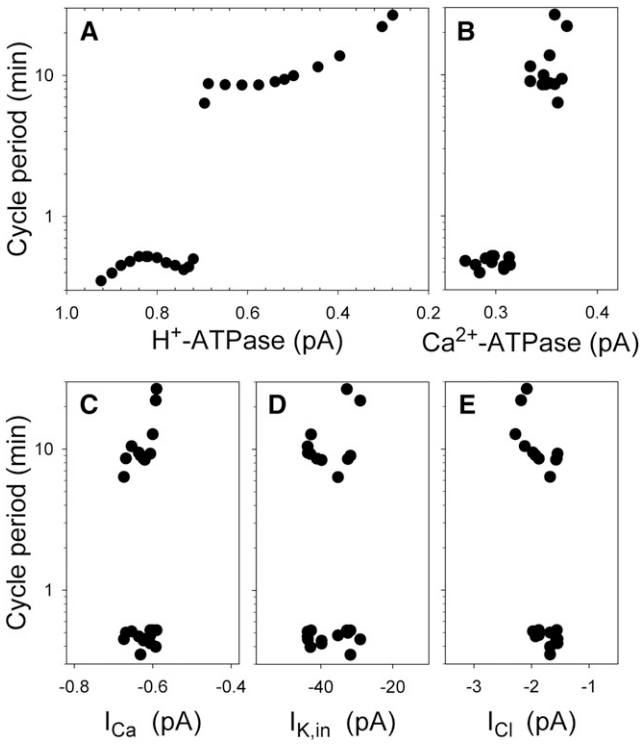

Figure 3. Oscillation cycle period is a well-defined function of H^+-ATPase activity but is largely independent of the Ca^{2+}-ATPase and the major channel currents at the plasma membrane. Data are from each of the longer oscillations in Figure 1 and from a selection of the short oscillations. A, H^+-ATPase current at 0 mV and the maximum hyperpolarization in the cycle. Note the discontinuity in cycle period around 0.7 pA. B, Ca^{2+}-ATPase current at 0 mV and minimum hyperpolarization in the cycle. C and D, Ca^{2+} I_{Ca} and $I_{K,in}$ currents at −200 mV and maximum hyperpolarization in the cycle. E, I_{Cl} current at −60 mV and minimum hyperpolarization in the cycle. Data for Mal^{2-} flux were equivalent to that for I_{Cl}, and for the outward-rectifying K^+ channels were complementary to those for $I_{K,in}$ and have been omitted from display.

an obvious correspondence to the cycle period (Fig. 3; Supplemental Fig. S1), and, of these pumps, only the H^+-ATPase is sensitive to $[Ca^{2+}]_i$ (Hills et al., 2012). Why a connection to the Ca^{2+}-ATPases should fail to surface is obvious when considering that, in the model, both of these pumps are much more strongly affected by changes in Ca^{2+} substrate availability, which varies by roughly 10-fold during the oscillations in $[Ca^{2+}]_i$. Thus, as Chen et al. (2012) noted before, it is the overall decline in energy-dependent transport activity following a period of solute accumulation—and specifically of the dominant H^+-ATPase—that is prerequisite to initiate the oscillatory behavior in the model.

We examined the effects of extracellular Ca^{2+} and K^+ concentrations that have been used to manipulate voltage and $[Ca^{2+}]_i$ and to drive their oscillations experimentally (Grabov and Blatt, 1999; Allen et al., 2001). Reducing extracellular Ca^{2+} to 0.1 mM in the model eliminated both voltage and $[Ca^{2+}]_i$ oscillations, leading to a much slower rate of stomatal closure. This behavior is entirely consistent with the requirement for Ca^{2+} entry to trigger endomembrane Ca^{2+} release and elevate $[Ca^{2+}]_i$ (Grabov and Blatt, 1998). Marginally higher external Ca^{2+} concentrations in the model returned $[Ca^{2+}]_i$ and voltage transients of irregular frequency spanning cycle periods of 8 to 85 min, and elevating external Ca^{2+} concentrations to 3 mM yielded sets of sharply defined oscillation frequencies and faster stomatal closure rates (Fig. 4). Analysis of closure rate as a function of oscillation period with 3 mM Ca^{2+} outside showed the most prominent of these was displaced to a cycle period near 12 min (=1.3 mHz), consistent with greater driving force for Ca^{2+} influx and the longer times needed to clear the cytosol of Ca^{2+} following each period of elevated $[Ca^{2+}]_i$. Varying extracellular K^+ concentration in the model, by contrast, had less impact on oscillation characteristics, although raising K^+ concentration broadened the range of the most prominent frequencies (Supplemental Fig. S2). This characteristic was primarily associated with the change in cycle number: over the range from 1 to 20 mM K^+, the model returned a difference in the total number of cycles that corresponds with the variation in the aperture differential between the open and closed pore at each concentration (Hills et al., 2012). With 1 mM or less K^+ outside, the model returned maximum apertures below 3 μm that closed to 1.8 μm with a single cycle in $[Ca^{2+}]_i$ elevation; in 20 mM K^+, the pore opened to more than 6 μm and closed to 1.8 μm with 14 cycles of $[Ca^{2+}]_i$ elevation. However, with 30 mM K^+, outside-the-membrane voltage situated positive of the range effective in promoting Ca^{2+} influx to trigger a rise in $[Ca^{2+}]_i$. As a result, the stomatal aperture closed only gradually. Again, these characteristics are broadly consistent with the very large body of literature on stomatal aperture and its dependence on external Ca^{2+} and K^+ (McAinsh et al., 1990; Fricker et al., 1991; Willmer and Fricker, 1996; Hills et al., 2012), and specifically with experimental manipulations of voltage and $[Ca^{2+}]_i$. Furthermore, the predictions of changes in oscillation period find direct support in experimental recordings, albeit in *Vicia* and *Commelina*, that show oscillation frequencies that varied with extracellular K^+ (Gradmann et al., 1993) and Ca^{2+} (McAinsh et al., 1995) concentrations. Most important, however, the analysis with different external Ca^{2+} and K^+ concentrations points to oscillation frequencies that are not immutable and are closely tied to the ionic drivers that contribute to flux across the plasma membrane.

Finally, we examined the consequences of altering the $[Ca^{2+}]_i$ sensitivity of the SLAC1 Cl^- current (I_{Cl}) on $[Ca^{2+}]_i$ oscillations and stomatal closure in simulation. A few recent studies have coined a new term "Ca^{2+} priming" (Kim et al., 2010), but the phenomenon it describes of modulation in $[Ca^{2+}]_i$ and other signal transduction processes—that is, of sensitivity control—is not new (see Trewavas [1992] and Berridge and Dupont [1994]; and for guard cells Armstrong et al. [1995], Grabov et al. [1997], Garcia-Mata et al. [2003], and Chen et al. [2010]). To date, meaningful kinetic data that describe the modulation of the $[Ca^{2+}]_i$ sensitivity of I_{Cl} are available only for the effects of protein phosphorylation

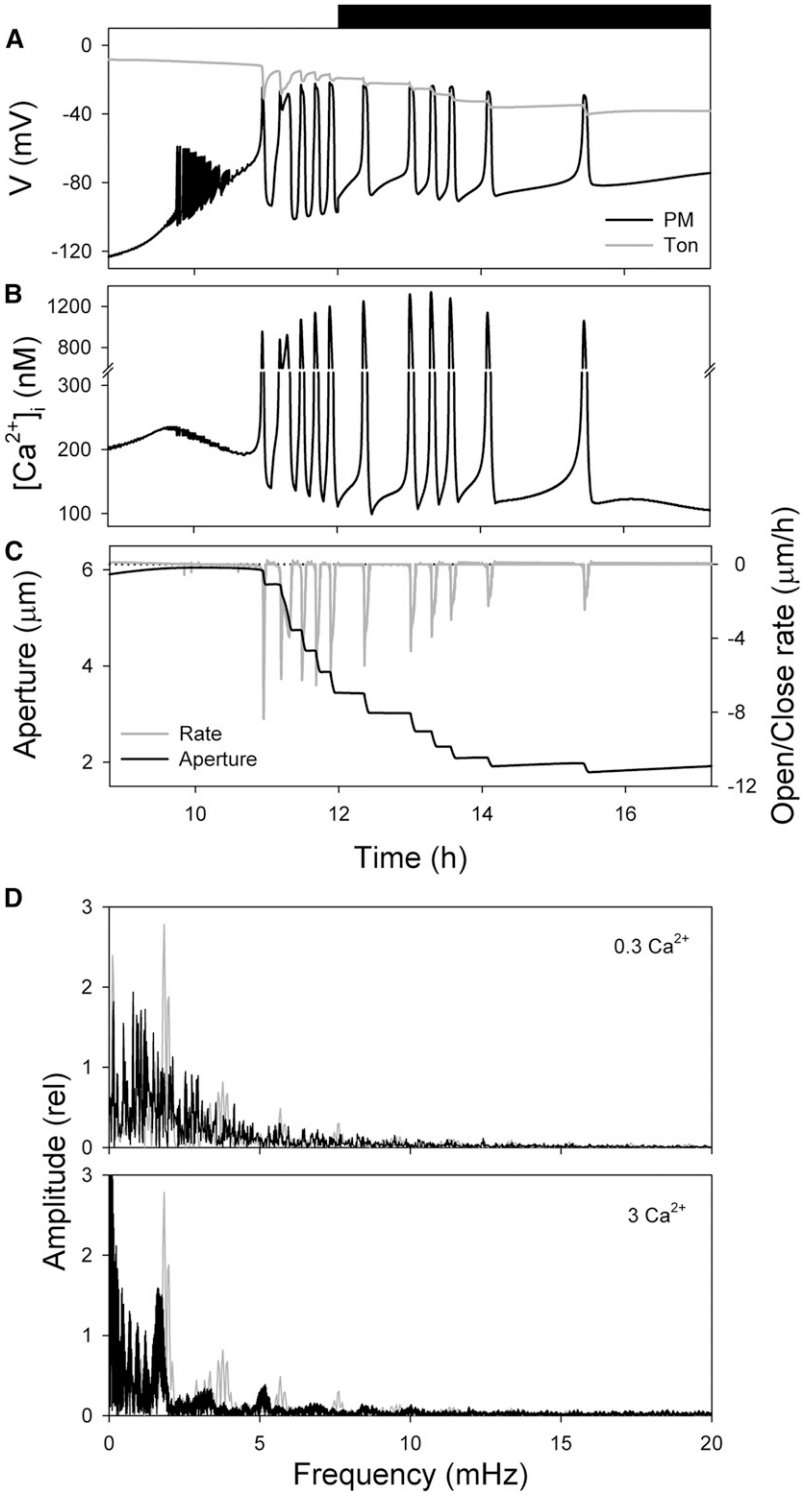

Figure 4. Outputs of the OnGuard Arabidopsis model with different extracellular Ca^{2+} concentrations. Outputs resolved as in Figure 1 but with 0.3 and 3 mM Ca^{2+} outside. A to C. Macroscopic outputs with 0.3 mM Ca^{2+} outside during the period from 8.8 to 17.2 h following the start of the diurnal cycle with plasma membrane and tonoplast voltage (A), $[Ca^{2+}]_i$ (B), and stomatal aperture and the rate of opening/closing in stomatal aperture (C; =ΔAperture/Δt). Positive rates here indicate opening, and negative rates indicate closing. Note the irregular oscillations in voltage and $[Ca^{2+}]_i$ and reduced rates of stomatal closure that extend into the dark period. Results with 3 mM Ca^{2+} are visually almost identical to those in Figure 1. D, Fourier analysis of oscillations in membrane $[Ca^{2+}]_i$ for the data in A to C and in with 3 mM Ca^{2+} outside. Data from Figure 1 are replotted in gray for reference. Note the loss in 0.3 mM Ca^{2+} of the prominent frequency near 1.9 mHz and the resolution of frequencies between approximately 0.5 and 1.8 mHz in 3 mM Ca^{2+}. Higher order resonance frequencies are also well-resolved near 3 and 5 mHz when Ca^{2+} is elevated outside.

in *Vicia* (Chen et al., 2010). These studies showed that protein phosphatase antagonism increases the $[Ca^{2+}]_i$ sensitivity of I_{Cl} with roughly a 200 nM reduction in the apparent K_{Ca} for activation of the current. In the Arabidopsis (*Arabidopsis thaliana*) model of OnGuard we examined so far, the K_{Ca} was set to 600 nM. As a test, we reduced this parameter to 400 nM and ran model again to generate the outputs in Figure 5. Compared to that in Figure 1, increasing the $[Ca^{2+}]_i$ sensitivity of I_{Cl} led to roughly a 20% reduction in the maximum aperture but had little effect on the maximum rate of stomatal closure. Most evident, however, was a halving in the number of cycles in $[Ca^{2+}]_i$ and voltage oscillations and a substantial lengthening of their periods. Fourier analysis (Fig. 5D)

showed that the prominent frequency of oscillations in $[Ca^{2+}]_i$ was displaced to a cycle period of 10.4 min (=1.6 mHz), some 2.5 min longer than observed with a K_{Ca} of 600 nM. In short, the effect of increasing the sensitivity of I_{Cl} to $[Ca^{2+}]_i$ was to extend the period of oscillations and reduce their number, but without substantial effect on closure rate. Thus, again, the results predict that the oscillation-frequency optimum is not immutable, that closure rate is not tied to a specific oscillation-frequency optimum, and that these frequencies depend on the ionic transporters that contribute to flux across the plasma membrane.

DISCUSSION

Chen et al. (2012) analyzed the mechanistic coupling between voltage, Ca^{2+} influx, and elevated $[Ca^{2+}]_i$ in detail and their connection to osmotic solute efflux during closure. They noted that membrane voltage is the common denominator that connects $[Ca^{2+}]_i$ with the osmotic solute flux. At its negative extreme, voltage favors K^+ and anion uptake but also triggers Ca^{2+} entry to elevate $[Ca^{2+}]_i$. At its positive extreme, voltage activates the channels mediating K^+ and anion efflux as well as engaging Ca^{2+}-ATPases to restore $[Ca^{2+}]_i$ to its resting level. Thus, the model gives quantitative understanding to a previous interpretation (Blatt, 2000) that the processes driving guard cell oscillations in vivo can be thought of as a cycle of four steps: (1) with resting $[Ca^{2+}]_i$ low, negative voltage triggers Ca^{2+} influx across the plasma membrane, stimulating endomembrane Ca^{2+} release to elevate $[Ca^{2+}]_i$; (2) the rise in $[Ca^{2+}]_i$ inactivates the Ca^{2+} channels, shuts down $I_{K,in}$ to prevent solute uptake, inactivates the H^+-ATPase, and

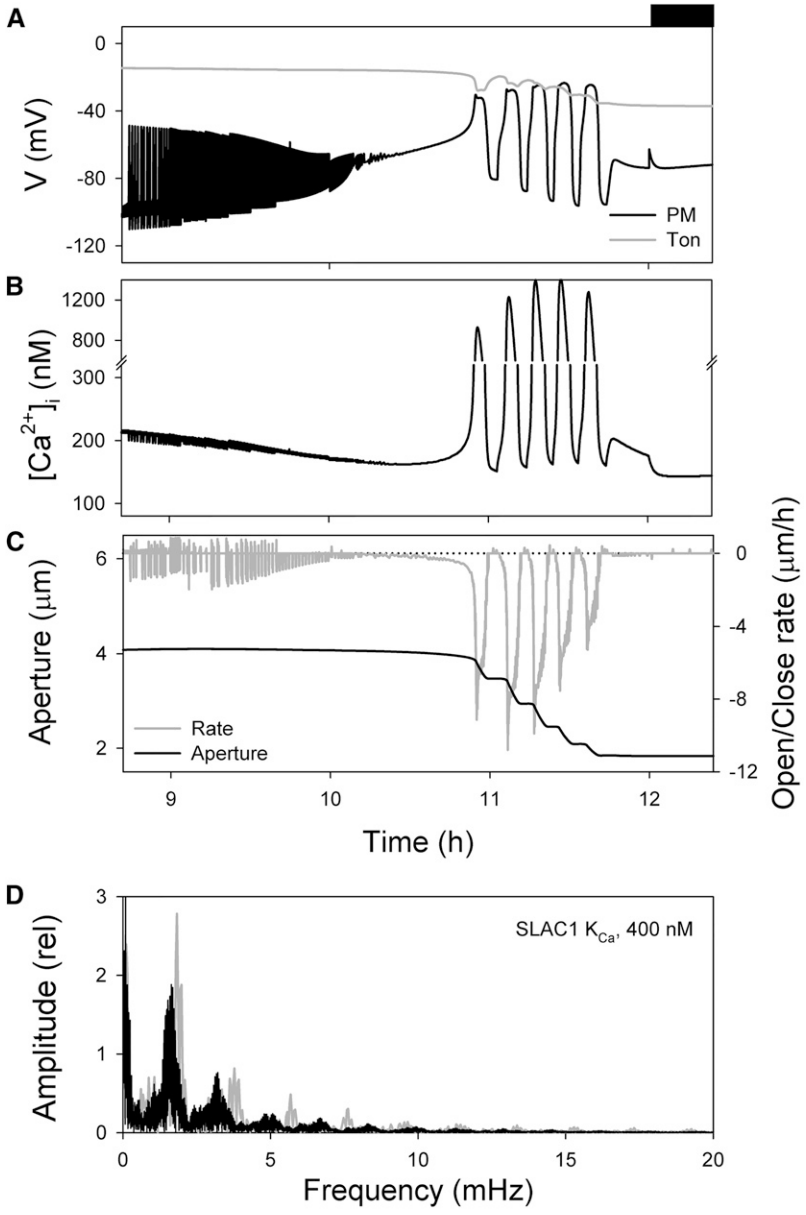

Figure 5. Outputs of the OnGuard Arabidopsis model with the $[Ca^{2+}]_i$ sensitivity of the SLAC1 Cl^- channel increased by reducing its K_{Ca} from 600 nM to 400 nM. Compare outputs with those resolved in Figure 1. A to C, Macroscopic outputs for the period from 8.7 to 12.4 h following the start of the diurnal cycle with plasma membrane and tonoplast voltage (A), $[Ca^{2+}]_i$ (B), and stomatal aperture and the rate of opening/closing in stomatal aperture (C; =ΔAperture/Δt). Positive rates here indicate opening, and negative rates indicate closing. Note the elongation in voltage and $[Ca^{2+}]_i$ oscillations and their reduction in number. D, Fourier analysis of oscillations in $[Ca^{2+}]_i$ for the data in A to C. Data from Figure 1 are replotted in gray for reference. Note the shift in prominent frequency to 1.6 mHz (=12.4 min). Higher order frequencies are also well-resolved and displaced to lower values.

activates I_{Cl} to promote membrane depolarization; (3) depolarization promotes K^+ and Cl^- efflux and, with Ca^{2+} influx suppressed, engages the Ca^{2+}-ATPases and CAX transporters to sequester Ca^{2+} and restore $[Ca^{2+}]_i$ to near-resting levels; and finally, (4) with the fall in $[Ca^{2+}]_i$, I_{Cl} declines, and $I_{K,in}$ and the H^+-ATPase recover sufficiently, the latter repolarizing the membrane to facilitate K^+ and H^+-coupled anion uptake. In short, voltage forms the core of this intrinsic feedback between membrane transporters operating across a common membrane. The cycle also incorporates a second feedback loop of $[Ca^{2+}]_i$-dependent controls on several of the major transporters that dominate osmotic solute flux and on the H^+-ATPase, not just on the Ca^{2+} channels at the plasma membrane and those facilitating endomembrane Ca^{2+} release. Our analysis of the SLAC1 Cl^- channel (Fig. 5) and variations in extracellular Ca^{2+} and K^+ concentrations illustrate a few of the predictions that arise from a quantitative analysis using OnGuard, and there are unquestionably others that can be drawn from similarly challenging these models. Overall, the most important and overarching of these is that voltage and $[Ca^{2+}]_i$ interact so as to oscillate in syncopation, driving with them K^+ and anion efflux to accelerate stomatal closure.

Even so, the existence of an optimal $[Ca^{2+}]_i$ oscillation frequency to drive stomatal closure is not obvious. Its emergence in simulation was entirely unexpected and underscores two points. First, the relationships between $[Ca^{2+}]_i$, voltage, and solute flux are highly nonlinear, as is amply demonstrated in the voltage-dependence of the component currents (Chen et al., 2012; Wang et al., 2012). Thus, only by quantitative systems analysis can the interactions between these different transporters, ion buffering and metabolism be fully understood. Second, analysis of the voltage and $[Ca^{2+}]_i$ oscillations exposes a close dependence on primary, ATP-dependent transport and the requirement in the model for its suppression to initiate and sustain the oscillations and accelerate stomatal closure. Clearly, the model predicts that the $[Ca^{2+}]_i$ and voltage oscillations are critically dependent on H^+-ATPase activity for their initiation and maintenance. It is difficult to assign an absolute value to the H^+-ATPase suppression needed for voltage and $[Ca^{2+}]_i$ to oscillate, but a rough estimate suggests values of 0.1- to 0.4-fold of the maximum pump output, in other words around 60% to 90% inhibition of the pump activity. The maximum current output of the modeled H^+-ATPase in Arabidopsis is approximately 2 pA per cell when $[Ca^{2+}]_i$ is 100 nM and the cytosolic pH is 7.6. So oscillations in voltage and $[Ca^{2+}]_i$ require that the pump output decline to roughly two-thirds or less of this value in order to enter the window of activity giving maximal stomatal closure rates (Figs. 2 and 3). If we consider the H^+ extrusion rates in Arabidopsis with fusicoccin and the *ost2* mutant to represent the maximum output—at which stomata do not close—then the H^+-ATPase activity of the wild type is within range of this estimate (Merlot et al., 2007), although clearly a value based on the mean output of the wild type represents an overestimate on H^+-ATPase activity permissive for rapid stomatal closure.

In summary, the simulations reported here provide a close match to experimental data that have indicated the coupling between voltage, the Ca^{2+} channels, and endomembrane Ca^{2+} release in driving the $[Ca^{2+}]_i$ cycle. Unexpectedly, OnGuard simulations support the perception that $[Ca^{2+}]_i$ oscillations associate with an accelerated rate in stomatal closure and that the most effective bandwidths fall within a narrow range of frequencies near 1.9 mHz (=8.9 min oscillation period) under our standard model conditions. What is all the more important, therefore, is that the model outputs offer a truly mechanistic basis from which to understand the origins of this frequency optimum. An analysis of the outputs does not support the perception that this frequency is in any way unique or that it acts to initiate or control a special signaling mechanism for osmotic ion efflux. Indeed, the range of oscillation frequencies in the model depends on the Ca^{2+} and K^+ concentrations outside, both in the model and published experiments, and the model predicts an oscillation frequency optimum that is subject to the Ca^{2+} sensitivity of the SLAC1 current. These observations underscore the lack of any uniqueness to the frequency optimum. All of the oscillations find their origins in the underlying relationships between voltage and current through each of the dominant transporters at the two membranes (Chen et al., 2012). More useful, then, is to recognize that the oscillations in voltage and $[Ca^{2+}]_i$ simply reflect a spectrum of frequencies that emerge from the balance of intrinsic transport activities of the guard cell, from their variation with H^+-ATPase and associated ATP-dependent transport activities, and from the several ionic driving forces across the guard cell membranes. It happens that the slower frequencies are sufficiently long-lived to enhance K^+, Cl^-, and Mal^{2-} efflux from the guard cells and accelerate stomatal closure. Whether the oscillatory output may signal other metabolic changes independent of transport, such as might depend on use- or frequency-encoded phosphorylation and gene expression (DeKoninck and Schulman, 1998; Flavell et al., 2006; Shalizi et al., 2006), remains an open question. What is clear, however, is that an optimum in $[Ca^{2+}]_i$ oscillations is a by-product, rather than a cause of, accelerated stomatal closure.

MATERIALS AND METHODS

Investigation of the modality of the $[Ca^{2+}]_i$ oscillations, their frequencies, link to stomatal dynamics, and mechanism, was carried out here on the Arabidopsis (*Arabidopsis thaliana*) version of the OnGuard model, briefly overviewed below. The study centered on the $[Ca^{2+}]_i$ oscillatory pattern spontaneously generated over a diurnal pattern under conditions detailed in the figures and text. Analysis of their origin, frequencies, and mechanism was carried out by a systematic examination of their correlation with plasma and tonoplast membrane voltages, stomatal aperture at different fluency regimes, and with the activities of the plasma membrane H^+- and Ca^{2+}-ATPases as well as $I_{K,in}$, $I_{K,out}$, I_{Ca}, I_{Cl}, and ALMT Mal^{2-} channels at the plasma membrane. Examination of the frequency components of the $[Ca^{2+}]_i$ oscillations was carried out by Fourier spectral analysis throughout.

Model Overview

A substantial body of data now exists that has led to an integrated and quantitative systems description of guard cells (Chen et al., 2012; Hills et al., 2012; Wang et al., 2012, 2014; Blatt et al., 2014). These quantitative models, generated with the OnGuard software (freely available at www.psrg.org.uk), codify the complexity inherent in the interactions between transport, metabolism, and buffering reactions of the guard cell, enabling a deep, mechanistic understanding inaccessible from intuition alone. OnGuard is built on user-definable libraries for transporter kinetics, chemical buffering, macromolecular binding, and metabolic reactions, and it includes the macroscopic equations essential to couple these processes to solute content, cell volume, turgor, and stomatal aperture (Hills et al., 2012). OnGuard models of *Vicia* and Arabidopsis reproduce the range of known properties of these guard cells with respect to ion transport, solute content, and stomatal aperture. They have yielded unexpected and emergent outputs, including counterintuitive changes in $[Ca^{2+}]_i$ and cytosolic pH over the diurnal cycle, and an exchange of vacuolar Mal^{2-} with Cl^- subject to the availability of the inorganic anion, all of which have direct support in independent experimental data (Raschke and Schnabl, 1978; MacRobbie, 1991, 1995, 2000, 2006; Thiel et al., 1992; Blatt and Armstrong, 1993; Willmer and Fricker, 1996; Frohnmeyer et al., 1998; Dodd et al., 2005, 2006). Furthermore, OnGuard models have demonstrated true predictive power, for example, in guiding experiments that led Wang et al. (2012) to explain how eliminating the SLAC1 Cl^- channel, which slows stomatal closure, also suppresses current through inward-rectifying K^+ channels to slow stomatal opening.

Model Construction

Construction of the *Vicia* and Arabidopsis models is detailed in previous publications (Chen et al., 2012; Hills et al., 2012; Wang et al., 2012; Blatt et al., 2014). Hills et al. (2012) provide a complete list of the transporters with short summaries of their characteristics, their parameterization, the associated genes and proteins, and details of sensitivity analyses (see Appendix 2 and Supplemental Tables 1 to 6 therein). For the present task, we used the Arabidopsis model (Wang et al., 2012) to analyze the $[Ca^{2+}]_i$ and voltage oscillations associated with stomatal closure. Again, Wang et al. (2012) provide the complete parameterization list for all of the transport and metabolic reactions in their supplemental material. In both models, the activities of all primary ATP-dependent transporters and organic solute synthesis in the guard cell are coupled to fluence rate. The activities of all other enzymatic, transport, and buffering processes are dictated by their inherent kinetics, binding, and regulatory parameters defined by the associated kinetic equations. Thus, the dynamic behavior of these transporters arises entirely from interactions between the component transport, buffering, and metabolic processes within the system as a whole. Oscillations in voltage and $[Ca^{2+}]_i$, which are observed in the models near the end of the daylight period shortly before and during stomatal closure, are a case in point. These oscillations follow on the decline in ATPase activities and reflect a release of the energy stored in the various ionic gradients that are generated during the daylight period. Chen et al. (2012) have analyzed the underlying mechanisms coupling voltage, Ca^{2+} influx and elevated $[Ca^{2+}]_i$ with osmotic solute flux during these oscillations in detail. This study also demonstrated that the simulated oscillations are a stable and reproducible feature of the diurnal cycle. Therefore, we focus here on the macroscopic characteristics of the oscillations, their frequency, and their dependence on extracellular Ca^{2+} and K^+ concentrations. The concentration parameters are directly accessible by the user in OnGuard and were employed previously to manipulate voltage and $[Ca^{2+}]_i$ experimentally, as noted above.

Supplemental Data

Supplemental Figure S1. Oscillation cycle period is a well-defined function of vacuolar VH^+-ATPase activity but shows little evidence of a dependence on the Ca^{2+}-ATPase or any of the major, $[Ca^{2+}]_i$-sensitive currents at the tonoplast.

Supplemental Figure S2. Fourier spectral analysis of oscillation frequencies in membrane voltage and $[Ca^{2+}]_i$ with 5 and 20 mM K^+ concentrations outside.

Received October 10, 2015; accepted December 1, 2015; published December 1, 2015.

LITERATURE CITED

Allen GJ, Chu SP, Harrington CL, Schumacher K, Hoffmann T, Tang YY, Grill E, Schroeder JI (2001) A defined range of guard cell calcium oscillation parameters encodes stomatal movements. Nature **411:** 1053–1057

Allen GJ, Chu SP, Schumacher K, Shimazaki CT, Vafeados D, Kemper A, Hawke SD, Tallman G, Tsien RY, Harper JF, et al (2000) Alteration of stimulus-specific guard cell calcium oscillations and stomatal closing in Arabidopsis det3 mutant. Science **289:** 2338–2342

Armstrong F, Leung J, Grabov A, Brearley J, Giraudat J, Blatt MR (1995) Sensitivity to abscisic acid of guard-cell K^+ channels is suppressed by abi1-1, a mutant Arabidopsis gene encoding a putative protein phosphatase. Proc Natl Acad Sci USA **92:** 9520–9524

Berridge MJ, Dupont G (1994) Spatial and temporal signalling by calcium. Curr Opin Cell Biol **6:** 267–274

Blatt MR (2000) Cellular signaling and volume control in stomatal movements in plants. Annu Rev Cell Dev Biol **16:** 221–241

Blatt MR, Armstrong F (1993) K^+ channels of stomatal guard cells: abscisic acid-evoked control of the outward rectifier mediated by cytoplasmic pH. Planta **191:** 330–341

Blatt MR, Garcia-Mata C, Sokolovski S (2007) Membrane transport and Ca^{2+} oscillations in guard cells. *In* S Mancuso, S Shabala, eds, Rhythms in Plants, Vol 1. Springer, Berlin, pp 115–134

Blatt MR, Thiel G, Trentham DR (1990) Reversible inactivation of K^+ channels of Vicia stomatal guard cells following the photolysis of caged inositol 1,4,5-trisphosphate. Nature **346:** 766–769

Blatt MR, Wang Y, Leonhardt N, Hills A (2014) Exploring emergent properties in cellular homeostasis using OnGuard to model K^+ and other ion transport in guard cells. J Plant Physiol **171:** 770–778

Chen ZH, Hills A, Bätz U, Amtmann A, Lew VL, Blatt MR (2012) Systems dynamic modeling of the stomatal guard cell predicts emergent behaviors in transport, signaling, and volume control. Plant Physiol **159:** 1235–1251

Chen ZH, Hills A, Lim CK, Blatt MR (2010) Dynamic regulation of guard cell anion channels by cytosolic free Ca^{2+} concentration and protein phosphorylation. Plant J **61:** 816–825

De Koninck P, Schulman H (1998) Sensitivity of CaM kinase II to the frequency of Ca^{2+} oscillations. Science **279:** 227–230

Dodd AN, Jakobsen MK, Baker AJ, Telzerow A, Hou SW, Laplaze L, Barrot L, Poethig RS, Haseloff J, Webb AAR (2006) Time of day modulates low-temperature Ca^{2+} signals in Arabidopsis. Plant J **48:** 962–973

Dodd AN, Love J, Webb AAR (2005) The plant clock shows its metal: circadian regulation of cytosolic free Ca^{2+}. Trends Plant Sci **10:** 15–21

Ehrhardt DW, Wais R, Long SR (1996) Calcium spiking in plant root hairs responding to Rhizobium nodulation signals. Cell **85:** 673–681

Flavell SW, Cowan CW, Kim TK, Greer PL, Lin Y, Paradis S, Griffith EC, Hu LS, Chen C, Greenberg ME (2006) Activity-dependent regulation of MEF2 transcription factors suppresses excitatory synapse number. Science **311:** 1008–1012

Fricker MD, Gilroy S, Read ND, Trewavas AJ (1991) Visualisation and measurement of the calcium message in guard cells. *In* W Schuch, G Jenkins, eds, Molecular Biology of Plant Development, Vol 1. Cambridge University Press, Cambridge, UK, pp 177–190

Frohnmeyer H, Grabov A, Blatt MR (1998) A role for the vacuole in auxin-mediated control of cytosolic pH by Vicia mesophyll and guard cells. Plant J **13:** 109–116

Garcia-Mata C, Gay R, Sokolovski S, Hills A, Lamattina L, Blatt MR (2003) Nitric oxide regulates K^+ and Cl^- channels in guard cells through a subset of abscisic acid-evoked signaling pathways. Proc Natl Acad Sci USA **100:** 11116–11121

Grabov A, Blatt MR (1998) Membrane voltage initiates Ca^{2+} waves and potentiates Ca^{2+} increases with abscisic acid in stomatal guard cells. Proc Natl Acad Sci USA **95:** 4778–4783

Grabov A, Blatt MR (1999) A steep dependence of inward-rectifying potassium channels on cytosolic free calcium concentration increase evoked by hyperpolarization in guard cells. Plant Physiol **119:** 277–288

Grabov A, Leung J, Giraudat J, Blatt MR (1997) Alteration of anion channel kinetics in wild-type and abi1-1 transgenic Nicotiana benthamiana guard cells by abscisic acid. Plant J **12:** 203–213

Gradmann D, Blatt MR, Thiel G (1993) Electrocoupling of ion transporters in plants. J Membr Biol **136:** 327–332

Hamilton DWA, Hills A, Blatt MR (2001) Extracellular Ba^{2+} and voltage interact to gate Ca2+ channels at the plasma membrane of stomatal guard cells. FEBS Lett **491:** 99–103

Hamilton DWA, Hills A, Kohler B, Blatt MR (2000) Ca^{2+} channels at the plasma membrane of stomatal guard cells are activated by hyperpolarization and abscisic acid. Proc Natl Acad Sci USA **97:** 4967–4972

Hills A, Chen ZH, Amtmann A, Blatt MR, Lew VL (2012) OnGuard, a computational platform for quantitative kinetic modeling of guard cell physiology. Plant Physiol **159:** 1026–1042

Keller BU, Hedrich R, Raschke K (1989) Voltage-dependent anion channels in the plasma membrane of guard cells. Nature **341:** 450–453

Kim TH, Böhmer M, Hu H, Nishimura N, Schroeder JI (2010) Guard cell signal transduction network: advances in understanding abscisic acid, CO_2, and Ca^{2+} signaling. Annu Rev Plant Biol **61:** 561–591

Kinoshita T, Nishimura M, Shimazaki K (1995) Cytosolic concentration of Ca^{2+} regulates the plasma membrane H^+ - ATPase in guard cells of fava bean. Plant Cell **7:** 1333–1342

Kwak JM, Mori IC, Pei ZM, Leonhardt N, Torres MA, Dangl JL, Bloom RE, Bodde S, Jones JDG, Schroeder JI (2003) NADPH oxidase AtrbohD and AtrbohF genes function in ROS-dependent ABA signaling in Arabidopsis. EMBO J **22:** 2623–2633

Lawson T, Blatt MR (2014) Stomatal size, speed, and responsiveness impact on photosynthesis and water use efficiency. Plant Physiol **164:** 1556–1570

Leckie CP, McAinsh MR, Allen GJ, Sanders D, Hetherington AM (1998) Abscisic acid-induced stomatal closure mediated by cyclic ADP-ribose. Proc Natl Acad Sci USA **95:** 15837–15842

Lemtiri-Chlieh F, MacRobbie EAC (1994) Role of calcium in the modulation of Vicia guard cell potassium channels by abscisic acid: a patch-clamp study. J Membr Biol **137:** 99–107

MacRobbie EAC (1991) Effects of ABA on ion transport and stomatal regulation. J Exp Bot **42:** 1–11

MacRobbie EAC (1995) Effects of ABA on 86 Rb^+ fluxes at plasmalemma and tonoplast of stomatal guard cells. Plant J **7:** 835–843

MacRobbie EAC (2000) ABA activates multiple Ca^{2+} fluxes in stomatal guard cells, triggering vacuolar $K^+(Rb^+)$ release. Proc Natl Acad Sci USA **97:** 12361–12368

MacRobbie EAC (2006) Osmotic effects on vacuolar ion release in guard cells. Proc Natl Acad Sci USA **103:** 1135–1140

McAinsh MR, Brownlee C, Hetherington AM (1990) Abscisic acid-induced elevation of guard cell cytosolic Ca^{2+} precedes stomatal closure. Nature **343:** 186–188

McAinsh MR, Webb A, Taylor JE, Hetherington AM (1995) Stimulus-induced oscillations in guard cell cytosolic-free calcium. Plant Cell **7:** 1207–1219

Merlot S, Leonhardt N, Fenzi F, Valon C, Costa M, Piette L, Vavasseur A, Genty B, Boivin K, Müller A, et al (2007) Constitutive activation of a plasma membrane H^+-ATPase prevents abscisic acid-mediated stomatal closure. EMBO J **26:** 3216–3226

Neill SJ, Desikan R, Clarke A, Hancock JT (2002) Nitric oxide is a novel component of abscisic acid signaling in stomatal guard cells. Plant Physiol **128:** 13–16

Pandey S, Zhang W, Assmann SM (2007) Roles of ion channels and transporters in guard cell signal transduction. FEBS Lett **581:** 2325–2336

Raschke K, Schnabl H (1978) Availability of chloride affects balance between potassium chloride and potassium malate in guard cells of Vicia faba L. Plant Physiol **62:** 84–87

Roelfsema MR, Hedrich R (2010) Making sense out of Ca^{2+} signals: their role in regulating stomatal movements. Plant Cell Environ **33:** 305–321

Shalizi A, Gaudillière B, Yuan Z, Stegmüller J, Shirogane T, Ge Q, Tan Y, Schulman B, Harper JW, Bonni A (2006) A calcium-regulated MEF2 sumoylation switch controls postsynaptic differentiation. Science **311:** 1012–1017

Staxen I, Pical C, Montgomery LT, Gray JE, Hetherington AM, McAinsh MR (1999) Abscisic acid induces oscillations in guard-cell cytosolic free calcium that involve phosphoinositide-specific phospholipase C. Proc Natl Acad Sci USA **96:** 1779–1784

Taylor AR, Manison N, Fernandez C, Wood J, Brownlee C (1996) Spatial organization of calcium signaling involved in cell volume control in the Fucus rhizoid. Plant Cell **8:** 2015–2031

Thiel G, MacRobbie EAC, Blatt MR (1992) Membrane transport in stomatal guard cells: the importance of voltage control. J Membr Biol **126:** 1–18

Trewavas AJ (1992) Growth substances in context: a decade of sensitivity. Biochem Soc Trans **20:** 102–108

Wang Y, Chen ZH, Zhang B, Hills A, Blatt MR (2013) PYR/PYL/RCAR abscisic acid receptors regulate K^+ and Cl^- channels through reactive oxygen species-mediated activation of Ca^{2+} channels at the plasma membrane of intact Arabidopsis guard cells. Plant Physiol **163:** 566–577

Wang Y, Hills A, Blatt MR (2014) Systems analysis of guard cell membrane transport for enhanced stomatal dynamics and water use efficiency. Plant Physiol **164:** 1593–1599

Wang Y, Papanatsiou M, Eisenach C, Karnik R, Williams M, Hills A, Lew VL, Blatt MR (2012) Systems dynamic modeling of a guard cell Cl^- channel mutant uncovers an emergent homeostatic network regulating stomatal transpiration. Plant Physiol **160:** 1956–1967

Webb AAR, McAinsh MR, Mansfield TA, Hetherington AM (1996) Carbon dioxide induces increases in guard cell cytosolic free calcium. Plant J **9:** 297–304

Willmer C, Fricker MD (1996) Stomata, Vol 2. Chapman and Hall, London, pp 1–375